Electric Current Sensors Employing Spun Highly Birefringent Optical Fibers

Richard I. Laming
David N. Payne

Reprinted from
JOURNAL OF LIGHTWAVE TECHNOLOGY
Vol 7, No. 12, December 1989

Electric Current Sensors Employing Spun Highly Birefringent Optical Fibers

RICHARD I. LAMING AND DAVID N. PAYNE

Abstract—**Highly elliptically birefringent fibers have been fabricated by spinning a linearly birefringent fiber during the draw. These fibers are particularly interesting for application as Faraday-effect fiber current monitors, since, in contrast with conventional fibers, they can be wound in small multiturn coils while retaining their sensitivity. The fiber and its exploitation in three optical schemes are modeled using Jones calculus and also experimentally investigated. A simple optical configuration is proposed, combining the elliptically birefringent fiber and a broad-spectrum light source. An accurate, compact, and robust current monitor is obtained. The sensor is characterized by a measurement repeatability of ±0.5 percent, a temperature drift of 0.05 percent/°C and a sensitivity of 1 mA rms/Hz$^{1/2}$. Further, we predict the performance of this sensor with optimized fiber length for a given measurement bandwidth.**

I. INTRODUCTION

SINCE THE early demonstrations of the principle of optical fiber current monitoring by Smith [1] and Papp *et al.* [2]–[4] there has been much research and development aimed at understanding the polarization properties of the fiber [5]–[16], developing optical signal processing schemes [17] and engineering a robust fiber-optic current sensor [18]–[20]. The main impetus for this work has come from the electrical power industry, since the fiber current monitor offers several advantages over conventional current transformers. Perhaps the most important of these is that the fiber is a dielectric and thus does not require the usual costly and bulky oil-filled electrical insulation tower, with its tendency to explode if breakdown occurs. This problem becomes more significant as transmission line voltages increase. A further advantage is that the fiber current sensor is able to detect transient electrical faults owing to its high measurement bandwidth, (limited only by the optical transit time of the light within the fiber). In addition, it is lightweight, small in size, and potentially less expensive.

The fiber current sensor consists of a coil of fiber wound around the current-carrying conductor, a light source, and a polarization analyzer [1], [2]. The Faraday effect causes a rotation of the plane of polarization of the light propagating in the fiber in proportion to the current flow. Analysis of the output plane of polarization therefore provides a measure of current.

The problem central to the development of a practical device is that of linear birefringence in the fiber, invariably present as a result of intrinsic manufacturing imperfections (core ellipticity, anisotropic stress) [16], [21] or induced by bending [11] and transverse pressure [13]. The linear birefringence interferes with the Faraday-induced rotation and even if present in small amounts makes it nearly unmeasurable. A simple rule is that the maximum usable fiber length in which Faraday rotation can be measured is one half of the fiber polarization beat length, defined as the length in which 2π phase slippage occurs between the two orthogonal linearly polarized modes of the fiber. Typical fibers have a beat length of a few meters when straight, or a few centimeters when packaged or wound in small coils. Thus whatever the length of the fiber employed in the current sensor coil (usual tens to hundreds of meters), the presence of linear birefringence can reduce the effective fiber interaction length to less than a meter. Moreover, packaging effects are environmentally unstable and this results in a variation in interaction length, and hence sensitivity, with time.

Early work to overcome the birefringence problem aimed at producing a low-birefringence fiber by spinning the preform during fiber drawing [6]–[9] to average the fast and slow birefringence axes. Such a fiber has been successfully commercially developed and has been widely used in experimental and prototype current monitors. However, when coiled the fiber suffers from bend-induced birefringence [11] which can catastrophically reduce the current sensitivity.

It has long been realized [10] that it is an indispensable requirement for measuring Faraday rotation to induce sufficient circular birefringence into the fiber to swamp the bend- and packaging-induced linear birefringence. The Faraday-induced rotation (a form of circular birefringence) then co-exists with the fiber intrinsic circular birefringence and is additive to it, thus allowing the full rotation to be measured.

Circular birefringence can be introduced into the fiber by torsional stress induced by twisting [10]. However, the number of turns per meter that the fiber can withstand before breakage (~ 100) limits the degree of circular birefringence which can be produced to a relatively low value and the fiber remains sensitive to the introduction of bend birefringence [8]. Thus the minimum coil size which can be wound is restricted to ~20-cm diameter. A further consequence is that the fiber has a long optical rotation length (typically 15 cm) and thus is sensitive to pressure which occurs over a length less than this. In par-

Manuscript received November 7, 1988; revised March 16, 1989.

The authors are with the Optical Fibre Group, Department of Electronics and Computer Science, The University, Southhampton, S09 5NH, U.K.

IEEE Log Number 8929394.

ticular, dynamic pressure caused by vibration has proved to be a severe problem [22].

Day [15] has tried to overcome the bending problem by annealing coiled fiber to remove the bend-induced birefringence. However, removal of the fiber coating and subsequent high temperature annealing tends to weaken the fiber, making it difficult to produce a small multiturn device. Moreover, the approach does not remove the vibration sensitivity.

Several attempts have been made to make fiber with a high intrinsic circular birefringence by introducing large permanent levels of torsional stress locked into the fiber by the cladding or a plastic jacket [23]. In another approach helical-core fibers [24], [25] have been developed which have exhibited optical rotation lengths as short as 4.9 mm. However, helical fibers tend to be awkward to handle because of their large diameter and asymmetric core; their use is thus restricted to large diameter coils.

In this work we describe a fiber that we believe is a complete solution to the problem, the spun elliptically birefringent (SEB) fiber [26], [27]. The fibers are made by spinning highly linearly birefringent [28] "bow-tie" preforms during the drawing process so as to impart a rapid built-in rotation of the fiber birefringent axes. The effect is that the fiber becomes elliptically birefringent. By careful choice of the spin rate relative to the pre-existing stress-induced linear birefringence, the resulting elliptically-polarized eigenmodes can be made quasicircular. In this case the fiber response to magnetic fields approximates that of an isotropic or circularly birefringent fiber. The advantage of the approach is that the fibers still retain a sufficiently large value of elliptical birefringence so as to impart a high resistance to external perturbations. The SEB can thus be regarded as a compromise between the polarization-holding (and consequent packaging insensitivity) of the highly linearly birefringent precursor fiber and the electric-current response of a true circularly birefringent fiber. This allows very small, multiturn coils to be wound and enables an extension of the sensitivity of fiber current monitors into the submilliamp region.

A disadvantage of the SEB fiber approach is that the precursor fiber depends for its linear birefringence on thermal stress [28], [29] and therefore the magnitude of the induced elliptical birefringence in the SEB fiber is temperature dependent.

We present here three signal processing schemes which successfully overcome the temperature problem. The advantages of each technique is discussed and the performance evaluated. A compact, sensitive, multiturn current sensor is described which is demonstrated to be vibration immune and have a temperature sensitivity of only 0.05 percent/°C. Consideration is also given to the limits of performance which might be attained by fiber current sensors.

II. Theory of Spun Fibers

The net birefringence [6], of a spun fiber of length z can be represented by two lumped birefringent elements, a retarder $R(z)$ with principal axis orientation $\phi(z)$ and a rotator $\Omega(z)$. The Jones matrix [30] describing the fiber is thus given by $[R]\,[\Omega]$, where

$$[R] = \begin{bmatrix} \cos\frac{R(z)}{2} + j\sin\frac{R(z)}{2}\cdot\cos 2\phi(z) & j\sin\frac{R(z)}{2}\cdot\sin 2\phi(z) \\ j\sin\frac{R(z)}{2}\cdot\sin 2\phi(z) & \cos\frac{R(z)}{2} - j\sin\frac{R(z)}{2}\cdot\cos 2\phi(z) \end{bmatrix} \tag{1}$$

and

$$[\Omega] = \begin{bmatrix} \cos\Omega(z) & -\sin\Omega(z) \\ \sin\Omega(z) & \cos\Omega(z) \end{bmatrix}. \tag{2}$$

The retardation and rotation of a length of fiber can be expressed in terms of the unspun linear birefringence $\Delta\beta$, spin twist rate ξ and Faraday-induced rotation angle per unit length f by

$$R(z) = 2\sin^{-1}\left(\frac{1}{(1+q^2)^{1/2}}\cdot\sin\gamma z\right) \tag{3}$$

$$\Omega(z) = \xi z + \tan^{-1}\left(\frac{-q}{(1+q^2)^{1/2}}\cdot\tan\gamma z\right) + n\pi \tag{4}$$

and

$$\phi(z) = \frac{\xi z - \Omega(z)}{2} + \frac{m\pi}{2} + \theta_{1s} \tag{5}$$

where

$$q = \frac{2(\xi + f)}{\Delta\beta} \tag{6}$$

$$\gamma = \frac{1}{2}\left(\Delta\beta^2 + 4(\xi + f)^2\right)^{1/2}. \tag{7}$$

m, n are integers and θ_{1s} is the initial orientation of the local slow axis of the fiber. Here $\phi(z)$ and θ_{1s} are defined with respect to vertical. In addition, it is assumed for these calculations that negligible torsional stress (i.e., post-draw twist) exists in the fiber.

The local Faraday rotation per unit length f for a fiber coil depends on its diameter D, the current I being passed through it and on the Verdet constant V of the fiber core. The Verdet constant of fused silica has been found to have a quadratic dependence on inverse wavelength [31]. From measurements made at wavelengths of 633 nm and 790 nm f can be expressed [1], [20] as

$$f = \frac{5.79\times10^{-19}}{\lambda^2}\frac{I}{D} \quad \text{(rad/m)}. \tag{8}$$

It is convenient now to introduce parameters which are derived from the previous formulas and which more

readily describe the fiber with respect to current sensing [26], [27], namely the elliptical polarization beat length L_p', and the normalized current sensitivity S. The elliptical polarization beat length L_p' can be expressed by

$$L_p' = \frac{L_p \cdot L_T}{(4L_p^2 + L_T^2)^{1/2} - 2L_p} \tag{9}$$

where the linear beat length L_p of the precursor fiber is

$$L_p = \frac{2\pi}{\Delta\beta} \tag{10}$$

and the spin pitch L_T is

$$L_T = \frac{2\pi}{\xi}. \tag{11}$$

The maximum fiber current sensitivity S normalized to the sensitivity of an ideal circularly birefringent fiber can be derived from (4) and is given by

$$S = \frac{4L_p^2/L_T^2}{1 + 4L_p^2/L_T^2}. \tag{12}$$

The actual value of fiber sensitivity found in practice depends on the optical configuration used (e.g., reflect back or single pass—see Section III). Here S represents the best case.

The normalized elliptical beat length and relative current sensitivity for the fiber are plotted in Fig. 1(a) and (b) as a function of the ratio of the spin pitch L_T to unspun linear beat length L_p. To make the fiber insensitive to external packaging effects we require the elliptical beat length L_p to be as short as possible. From Fig. 1(a) we see that this is achieved by choosing a starting preform with short unspun linear beat length L_p and then selecting a large ratio of spin pitch to unspun linear beat length. However, this ratio cannot be increased indefinitely as the effect is a large decrease in the relative fiber current sensitivity (Fig. 1(b)). The decreased sensitivity results because the ellipticity of the eigenmodes of the fiber becomes greater and approaches that of a high linearly-birefringent fiber (i.e., linearly polarized modes). It is well known that such a fiber has a very small response to current. We must therefore choose a compromise between the two parameters and obtain as short an elliptical mode beat length as possible without seriously reducing the sensitivity. An optimized fiber might have a spin pitch approximately equal to the unspun linear beat length, and is thus quasicircularly birefringent with $L_p' \approx 4.2L_p$ with relative fiber current sensitivity S around 80 percent (see points marked on Fig. 1(a) and (b)). If we start with a typical unspun bow-tie preform having a fiber beat length of 1 mm, a spun fiber having an elliptical beat length of 4.2 mm will result. This degree of elliptical birefringence is very high and sufficient to allow a bend radius as small as 5 mm (see Section III-C).

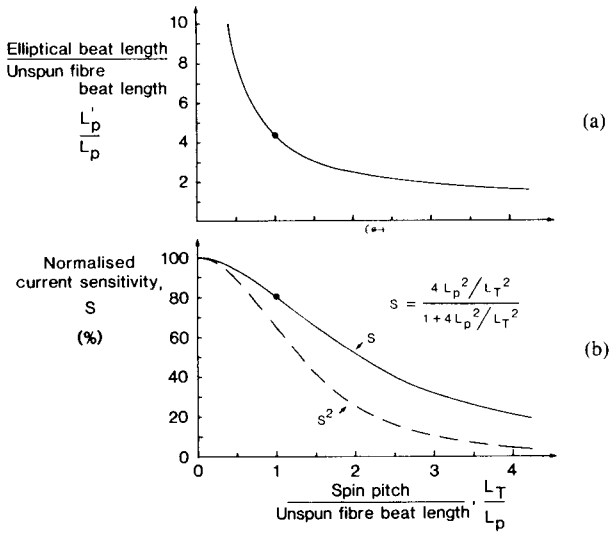

Fig. 1. (a), (b) Normalized elliptical beat length and relative current sensitivity as a function of the ratio of spin pitch to unspun fiber beat length.

III. Current Sensors Using SEB Fiber

Most fiber current-sensor measurement schemes use a configuration which involves launching linearly polarized light into the fiber and analyzing the state of polarization of the output. In the case of an isotropic or pure circularly birefringent fiber the output is plane polarized and rotated by the Faraday effect. For an SEB fiber which is quasi-circularly birefringent, the fiber can be regarded as composed largely of a rotator element, but with a small retarder component. The output state of polarization (SOP) then will be in general nearly plane-polarized, with a degree of polarization ellipticity which depends on how close to circularly birefringent the fiber has been designed. Since SEB fiber is obtained by spinning a fiber with thermal stress-induced linear birefringence, the magnitude of the resultant elliptical birefringence is also temperature dependent. The following optical configuration schemes were developed to compensate for the varying polarization orientation and ellipticity which results from the temperature-sensitive elliptical birefringence.

A. Scheme 1: Active Temperature Compensation

The approach is shown schematically in Fig. 2. Polarized output from a monochromatic laser is launched into the fiber coil. The output from the coil is passed through a polarization controller which compensates the slow temperature-dependent birefringence changes in the fiber. The polarization controller does not respond to the higher-frequency current-induced polarization changes and therefore the processed electrical output is a direct measurement of current. The use of an integrator in the polarization controller feedback loop ensures that the output SOP is nominally linear at an angle of 45° to the axis of the polarization beamsplitter and thus a stable, accurate current measurement is obtained.

The scheme was implemented with an all fiber polarization controller [32]. Maximum current sensitivities of

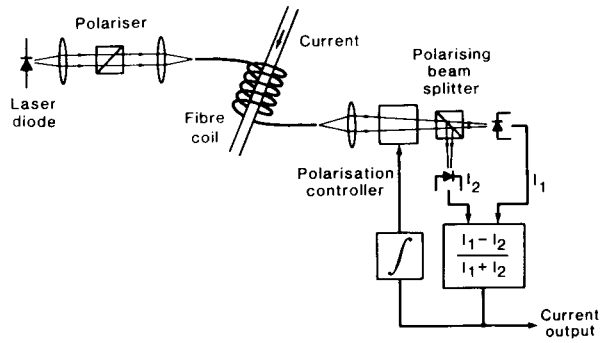

Fig. 2. Scheme 1: Active temperature compensation.

100 μA rms/Hz$^{1/2}$ for an 80-turn sensor operating at 633 nm (HeNe), and 100 μA rms/Hz$^{1/2}$ for a 185 turn sensor operating at 790 nm (diode laser), were obtained. However, it was found that since the fiber birefringence is wavelength sensitive, a narrow spectrum light source (<1 GHz) was required to ensure a polarized output. For the semiconductor-powered sensor the frequency jitter [33], [34] of the laser emission wavelength caused polarization noise at the output of the sensor, reducing its maximum sensitivity at frequencies below ~ 100 kHz.

B. Scheme 2: Orthoconjugate Reflector

An orthoconjugate reflector (OCR) [35], which consists of a 45° Faraday rotator and mirror has previously been proposed as a means of returning the orthogonal polarization-state back down a fiber such that all reciprocal linear and circular birefringence in the fiber is undone. The returning polarization state will then always be linear and orientated at 90° to the launch state. However, a nonreciprocal rotation in the fiber due to current-induced Faraday rotation will add on the return pass and will not be undone by the OCR. A double Faraday rotation will thus be observed.

An experimental current sensor utilizing this technique was constructed and is shown schematically in Fig. 3. Polarized light from a single longitudinal mode semiconductor laser operating at 780 nm was launched through a polarization insensitive beamsplitter into the fiber coil. The output from the coil was collimated and passed through a bulk 45° Faraday rotator, reflected by a mirror, passed back through the rotator and relaunched into the fiber. The polarization state is thus rotated by 90° (i.e., orthogonal to itself) before reinsertion into the fiber. The returned light is deflected by a polarization-insensitive beamsplitter and analyzed with a polarizing beamsplitter. The ratio output provides a measure of the current since the returned polarization is rotated by double the nonreciprocal Faraday-induced rotation in the fiber.

A 30-turn loosely wound fiber coil of ~ 20-cm diameter was used, wound from fiber of 100-μm diameter, 0.14 NA having unspun linear beat length $L_p = 1.62$ mm and spin pitch $L_T = 1.64$ mm. This gave an elliptical beat length $L_p' = 6.8$ mm and projected relative current sensitivity $S = 79.6$ percent.

The sensor response to current was measured while increasing the temperature in the range 20 to 70°C and it was found that the OCR stabilized the current reading significantly. Without the OCR a variation in sensitivity of $\sim \pm 25$ percent was obtained, whereas with it rapid sensitivity oscillations of ± 2 percent occurred around the measured nominal 77 percent relative sensitivity. The remaining variations were due to residual, imperfectly compensated linear birefringence in the fiber which varies with temperature.

Although providing an interesting compensation, the OCR is bulky, temperature sensitive in itself, and requires shielding from magnetic fields. It would thus be necessary to incorporate it into the terminal equipment.

C. Scheme 3: Reflect-Back Configuration

The reflect-back configuration in which a mirror is placed at the end of the fiber has been suggested previously [36] as a method of compensating the thermal variations in the twist-induced circular birefringence experienced in a current monitor which utilizes twisted low-birefringence fiber. In the SEB fiber current-monitor the scheme has a similar effect in compensating variations in the dominant circular birefringence component of the fiber, but unfortunately not in the linear birefringence component.

1) Principle of Operation: A schematic diagram of the reflect-back SEB fiber current sensor [37], [38] is shown in Fig. 4. Light output from a semiconductor light source is polarized at 45° to the vertical and launched through a polarization-insensitive beamsplitter into the fiber coil. Light at the far end of the fiber coil is reflected by a mirror and passes back through the coil where it is directed by the polarization-insensitive beamsplitter to an analyzer consisting of a polarizing beamsplitter orientated with axis vertical and horizontal.

The reflect-back current monitor can be modeled by Jones calculus [30] as

$$\begin{bmatrix} E_x \\ E_y \end{bmatrix}_{\text{OUT}} = \frac{1}{\sqrt{2}} [R'][\Omega'][\Omega][R] \begin{bmatrix} 1 \\ 1 \end{bmatrix} \tag{13}$$

where $[R]$, $[\Omega]$ are the forward lumped retarder and rotator elements given in (1) and (2), and $[R']$, $[\Omega']$ are the elements seen in the reverse direction. Note that $[\Omega']$ must have its sign reversed to allow for phase reversal of the mirror and is therefore given by

$$[\Omega'] = \begin{bmatrix} \cos \Omega'(z) & \sin \Omega'(z) \\ -\sin \Omega'(z) & \cos \Omega'(z) \end{bmatrix}. \tag{14}$$

The values of $R'(z)$, $\Omega'(z)$ and $\phi'(z)$ required for calculation of $[R']$ and $[\Omega]$ can be found from (3)–(8), with the sign of the Faraday-induced rotation per unit length f reversed to allow for the nonreciprocal nature of the Faraday effect. We can now calculate the output response P

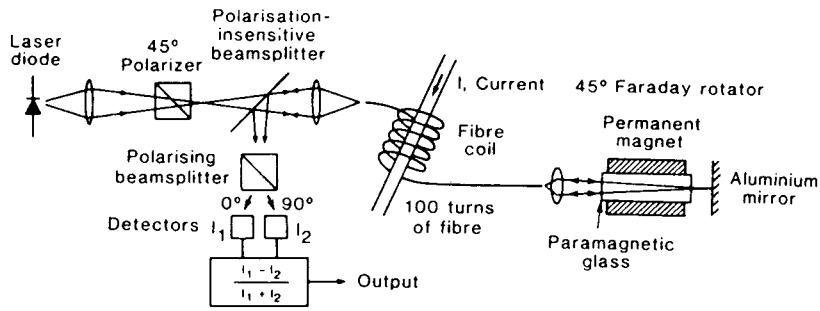

Fig. 3. Scheme 2: Orthoconjugate reflector.

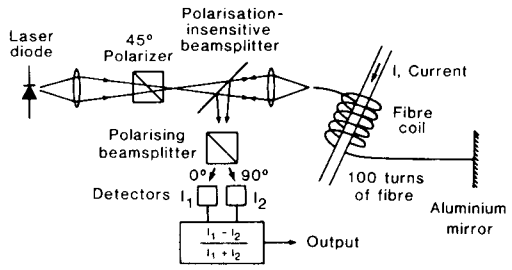

Fig. 4. Scheme 3: Reflect-back configuration.

from the ratio electronics [18]

$$P = \frac{I_1 - I_2}{I_1 + I_2} = \frac{E_x^2 - E_y^2}{E_x^2 + E_y^2} \tag{15}$$

and the normalized current sensitivity s (defined as the ratio of the incremental responses dP/di to current flow i for spun and ideal fibers) as a function of thermal changes in birefringence L_p. The theoretical results for a 10-m fiber are as plotted against birefringence (and approximate temperature [29]) for several orientations of the fiber at the input, θ_{1s} in Fig. 5(a) and (b). The fiber has a spin pitch $L_T = 1.64$ mm ($\xi = 1219\pi$ rad $\cdot$ m^{-1}) and nominal linear beat length, $L_p = 1.62$ mm ($\Delta\beta = 1234\pi$ rad $\cdot$ m^{-1}). The response P varies widely with increasing temperature and depends on fiber orientation θ_{1s}. The small-signal current sensitivity s has a much smaller variation ($\sim$25 percent) and is identical for all input angles. Note that the peak value of s (79.6 percent) corresponds to the maximum sensitivity S calculated from (12).

Fig. 5(c) and (d) shows experimentally determined response and sensitivity curves for a loosely wound, 30-turn fiber coil with nominal unspun linear beat length L_p = 1.62 mm and spin pitch L_T = 1.64 mm. The total fiber length was $\sim$10 m and a single-longitudinal mode semiconductor laser operating at 780 nm was used to inject light into the fiber with a polarization orientation $\theta_{1s} \approx 110°$. The results are in excellent agreement with the theoretical predictions.

Although much reduced by use of the reflect-back scheme, the oscillations in current sensitivity ($\pm$25 percent) remain unacceptable. However, it was found that they can be considerably reduced by employing a broad-spectrum light source to average the variations. The effect can be understood as follows. Let us consider passing a

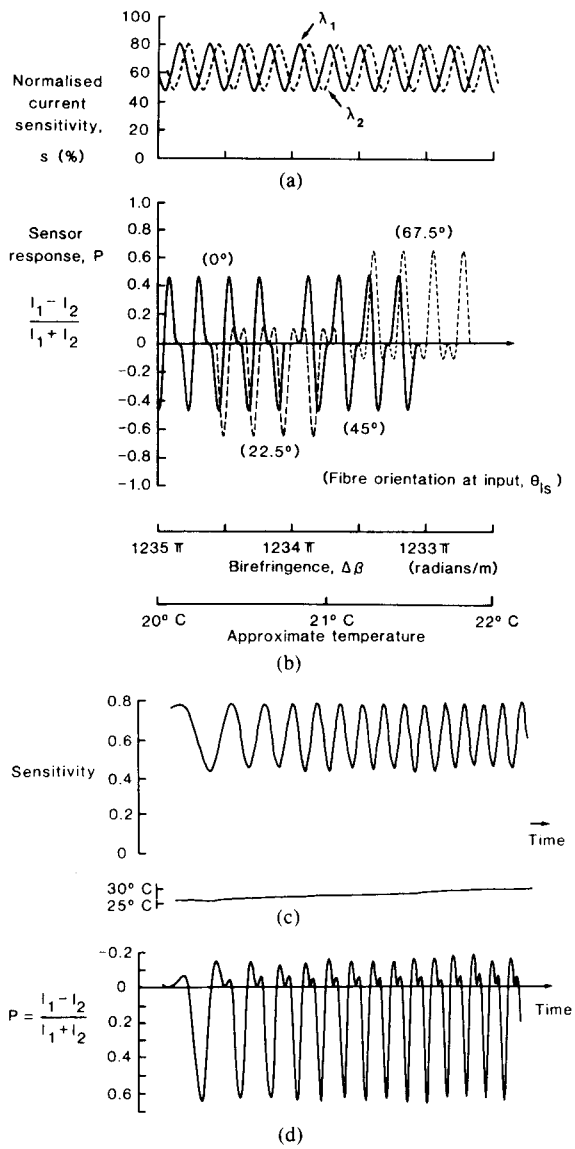

Fig. 5. (a), (b) Theoretical sensitivity s and response P curves for an SEB current sensor having spin rate ξ = 1230 rad/m plotted against thermal variations in unspun birefringence. (c), (d) Experimental sensitivity s and response P curves obtained while varying the sensor temperature.

second wavelength λ_2 simultaneously through the fiber. The sensitivity and response oscillations will be shifted slightly in phase as shown by the dashed curve in Fig. 5(a). Thus if the spectrum of the source contains a continuum of wavelengths the curves will be smoothed to a

value corresponding to the mean of the oscillations. For the example used here the sensitivity will be averaged to a nominal 63.5 percent of the ideal current sensor (see below). To achieve complete averaging it is necessary for the source to have a spectral width such that its coherence length is about one tenth of the path length difference between polarized modes. For the above experimental values a spectral width of ~ 5 nm would suffice.

The spectral averaging effect was experimentally verified by repeating the experiment while reducing the drive current in the single longitudinal mode semiconductor laser until it behaved as an ELED. Simultaneously, the coil temperature was continuously increased. The results are shown in Fig. 6 where the fiber current sensitivity is compared in time with the fiber temperature. The plot shows a dramatic reduction in sensitivity variations with temperature once the laser begins operating as a broad spectrum ELED.

It should be noted that the use of spectral averaging reduces the current sensitivity from the maximum obtainable S (equation (12)) to a value given by S^2. This expression is plotted in Fig. 1 for comparison with the single-pass narrow-spectrum fiber sensitivity. It can be seen that the current sensitivity at the desired operating point of $L_T/L_p = 1$ is 64 percent.

2) Minimum Permitted Coil Diameter: The effect on current sensitivity of coiling an SEB fiber can be approximately modeled by considering the fiber as truly circularly birefringent with optical rotation length equal to twice the elliptical beat length. The bend-induced linear birefringence induces a linear beat length L_B in the plane of the bend [11], where

$$L_B = \frac{7.4\lambda \cdot D^2}{d^2}. \tag{16}$$

Here D and d are the coil and fiber diameters, respectively. The optical rotation-length and bend-induced linear beat length L_B are analogous with spin-pitch L_T and unspun linear beat length L_p of (10) and (11). We can therefore use the previously developed expression for S^2 (equation (12)) to give a sensitivity when bent S_B^2, where

$$S_B = \frac{L_B^2/L_p'^2}{1 + L_B^2/L_p'^2}. \tag{17}$$

The total current sensitivity of a coiled spun Hi-Bi is then approximated by the product of S^2 and S_B^2.

A 92-μm-diameter fiber with unspun linear beat length $L_p = 2.05$ mm and spin pitch $L_T = 1.49$ mm was used for the bend sensitivity measurements. The fiber elliptical beat length L_p' was therefore 11.5 mm, giving a predicted current sensitivity S^2 of 78 percent. Experimentally the current sensitivity was measured to be 80 percent of an ideal fiber.

The fiber was loosely coiled into sensors of diameters 50, 40, 25, 17, and 12 mm. The normalized current sensitivities measured for the different diameters are plotted in Fig. 7 along with S_B^2. The experimental data and theoretical curve are in good agreement and it can be seen that this particular fiber can be continuously coiled to a diameter of 13 mm before a current sensitivity reduction of 1 percent occurs. If the fiber were designed with shorter elliptical beat length or smaller diameter (to reduce bend birefringence) the minimum radius could be made much smaller. A practical limit of a few millimeters coil diameter is possible.

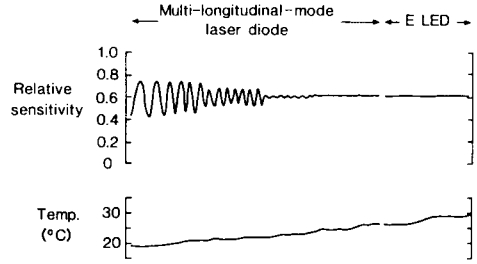

Fig. 6. Improvement in current sensitivity variations with temperature due to increasing spectral width of the source.

IV. Tests on a Prototype Reflect-Back SEB Current Sensor

A prototype current sensor was constructed based on the design outlined above. A 100 turn 25-mm diameter coil was wound on a silica former. The fiber had a diameter of 100 μm and measured parameters of unspun linear beat length $L_p = 1.7$ mm and spin pitch $L_T = 1.64$ mm resulting in an elliptical beat length L_p' of 7.44 mm. The computed fiber current sensitivity S^2 is thus 66 percent of an ideal fiber.

A General Optronics superluminescent diode (SLD) was used as the light source. The SLD had a broad-spectrum emission with a FWHM of 12 nm centered at 821 nm. The device was pigtailed and gave a relatively low power output (0.1 mW) into a single-mode fiber compared with present commercially available SLD's. The coil attenuation was less than 0.3 dB.

The sensor response was characterized for long-term drift, temperature stability, fiber input-angle sensitivity, applied pressure on the fiber, vibration sensitivity and large and small signal response.

A. Long-Term Stability

A signal current of 10-A rms at 488 Hz was passed through the sensor coil. The sensor response in a laboratory environment was measured with a lock-in amplifier having a time constant of 0.3 s and the data logged by a computer every 0.5 s for 1 h. The recorded data is shown in Fig. 8. It can be seen that the averaged fiber current sensitivity is 67.25 percent of an ideal circularly birefringent fiber (in good agreement with the theoretically predicted value of 66 percent). The maximum deviation of the data from this mean was ± 0.3 percent of the mean value with a standard deviation 0.085 percent.

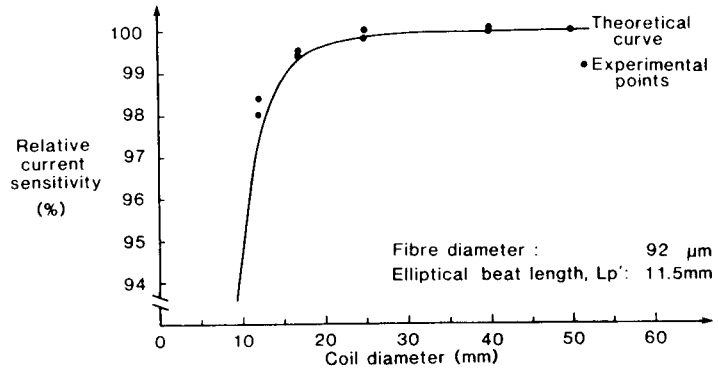

Fig. 7. Effect of coil diameter on fiber current sensitivity.

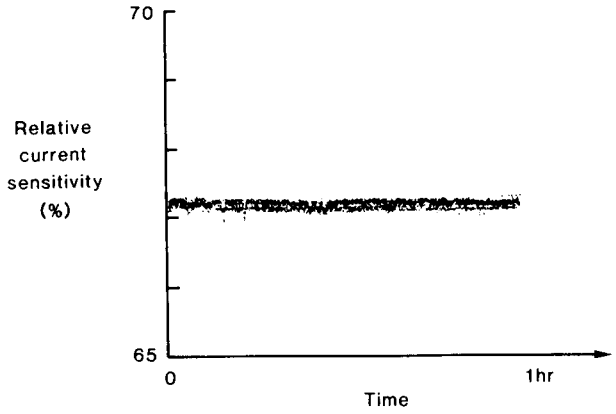

Fig. 8. Long-term drift in current sensitivity.

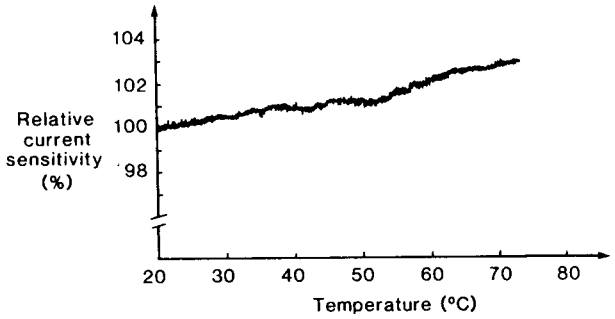

Fig. 9. The effect of temperature on the sensor response.

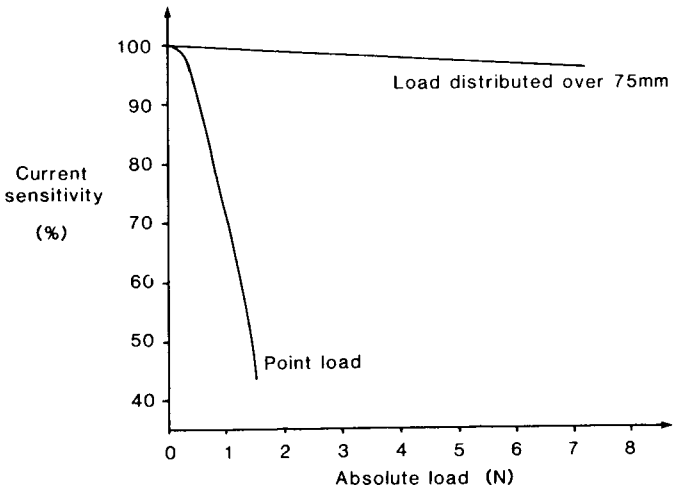

Fig. 10. Variation in current sensitivity with applied load on the fiber.

B. Temperature Sensitivity

The sensor response to current was measured as a function of temperature in the range 20–70°C. The data, normalized to a sensor response of 67 percent, is shown in Fig. 9. It was found that the current sensitivity increased linearly by ~ 0.05 percent/°C. This is expected and is due to the linear birefringence component $\Delta\beta$ decreasing (L_p increasing) with temperature (see (12)). Although a very acceptable figure, further improvements are possible by using a fiber with less temperature sensitive birefringence, such as an elliptical-core fiber.

C. Input Angle

The sensor current sensitivity was measured as a function of fiber input angle between 0° and 90° and was found to be independent of input angle within the measurements accuracy of ± 0.5 percent.

D. External Forces

The effect on sensor response of lateral side pressure applied to the fiber was investigated by applying a distributed load to a 75-mm straight portion of fiber at the mirror-end of the coil. The fiber was 100 μm in diameter and coated to a diameter of 200 μm.

The current sensitivity is plotted against absolute load in Fig. 10 for uniformly distributed and point load. It can be seen that a distributed load of $2N$ reduced the sensitivity to 99 percent of its full value. If applied to a low-birefringence fiber of similar diameter, this would result in induced linear birefringence of 45° [13] and would catastrophically destroy the response of a conventional fiber-optic current monitor [18]. This clearly demonstrates the advantages of SEB fiber over standard single-mode fiber.

As expected, the very high point load affects the sensor strongly, since it is localized to a length shorter than the optical rotation in the fiber and is therefore not averaged. This severe test shows that even highly birefringent fibers have a limit to their polarization-holding ability.

E. Vibration Test

A vibration applied locally to a fiber or, more specifically, to an SEB fiber, can introduce additional local linear birefringence, or can modify the local unspun linear-birefringence $\Delta\beta$. Referring to the theoretical curves of absolute fiber output P against birefringence $\Delta\beta$ (Fig. 5(b)) for a monochromatic source, it can be seen that any change in birefringence causes a change in the sensor output which is indistinguishable from actual current. Whereas this is a serious problem in conventional fiber current monitors, the broad-spectrum source smoothes the output-ratio dependence on fiber birefringence and thus significantly reduces the vibration sensitivity.

A section of fiber from the mirror-end of the coil was attached with contact adhesive to the top surface of a 0.5″ accelerometer, as shown in Fig. 12(a). The fiber was subjected to controlled lateral vibrations over the frequency range 30 Hz–1 kHz and the induced current signal was measured. The test was repeated on low-birefringence fiber of similar dimensions.

The vibration sensitivity of the two fiber types are shown in Fig. 11(b), where the vibration-induced effective current for 1 g of applied acceleration is plotted against the vibration frequency. The vibration sensitivity of low-birefringence fiber was large and, as expected, dependent on the orientation of applied vibration. However, owing to the strong elliptical birefringence present in the SEB fiber and spectral averaging, its vibration sensitivity was reduced by approximately 40 dB and found to be insensitive to the orientation of applied vibration.

The sensitivity of SEB fiber was found to be approximately 40 dB lower than low-birefringence fiber. The sensitivity decreased with increasing frequency, but was not proportional to applied displacement, as might be anticipated.

At a frequency of 50 Hz a current of 50 mA would be measured if the fiber were subjected to an acceleration of 1 g. Moreover, the experimental fiber was loose wound and a carefully-packaged sensor could be expected to have a much lower vibration sensitivity.

F. Maximum Sensitivity

Oscilloscope traces of the 100-turn sensor noise output and response to a signal current of 1 A rms at 25 Hz are shown in Fig. 12 for a measurement bandwidth of 1 kHz. The maximum sensitivity was detector shot-noise limited to 1 mA rms/$Hz^{1/2}$ as a result of the low power available from the SLD and excess optical losses in the bulk components. A more powerful light source and refinement of the optics should result in a maximum sensitivity of 100 μA rms/$Hz^{1/2}$, or 10 mA turn/$Hz^{1/2}$.

G. Large-Signal Current Response

The sensor response $(I_1 - I_2/I_1 + I_2)$ to current is a sine function. Thus it is intrinsically nonlinear and has been evaluated numerically by solving the matrix equations (13) which model the polarization behavior of an SEB fiber, as well as that of conventional fibers.

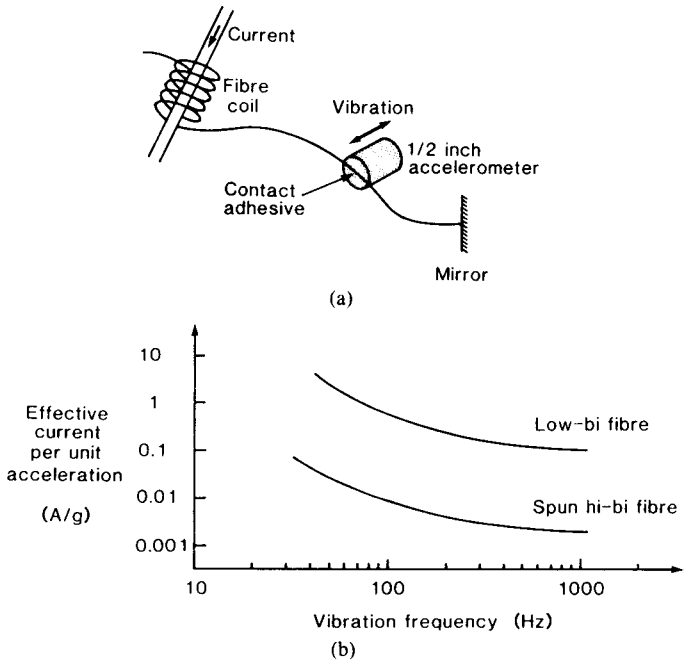

Fig. 11. (a), (b) Induced current due to vibration.

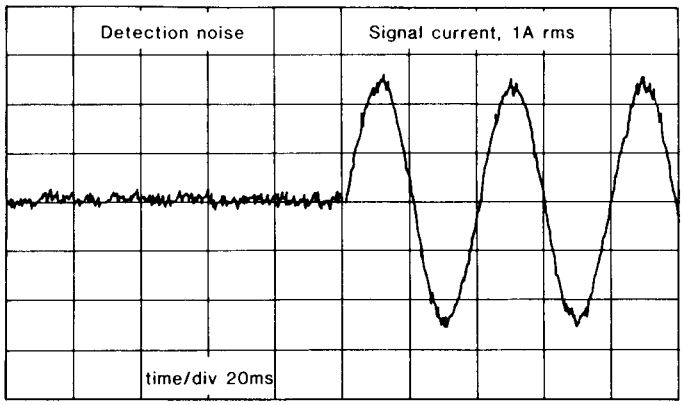

Fig. 12. Current response of 100 turn fiber coil of 25-mm diameter.

The absolute sensor response for several input angles is shown in Fig. 13, and compared to that of an ideal circularly-birefringent fiber. The response is sinusoidal and has a small dc-offset, the magnitude of which depends on fiber orientation. Note that the small signal sensitivity (i.e., incremental) will not be affected by the dc offset and will be invariant with orientation. It can be seen that as the current increases towards ± 1500 A the sensitivity to current decreases. This limits the maximum current range of the 100 turn sensor to ± 1.5 kA, or, more practically, to approximately 500 A for 5-percent linearity. It can be seen that this limit is $S^{-1/2}$ times higher than that for a similar coil of ideal fiber.

H. Experimental

The large signal response was evaluated by passing current in the range 20–450 A rms at 50 Hz through the sensing coil. The response was measured with a lock-in am-

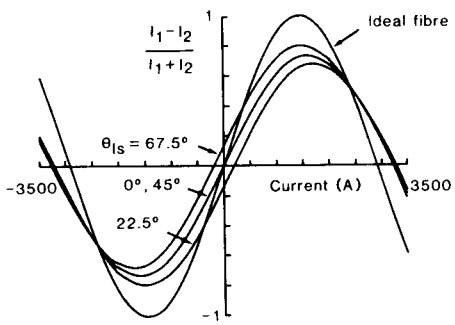

Fig. 13. Calculated large-signal response of SEB fiber compared with that of the ideal fiber.

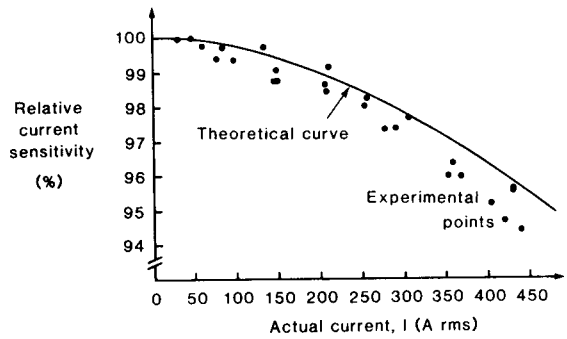

Fig. 14. Relative large-signal response of SEB fiber current sensor.

plifier which responded only to the fundamental frequency component ω of the signal. As the sensor response and the signal are both sinusoidal, the theoretical normalized response $P(\omega)$ as a function of current is given by a Bessel expansion:

$$P(\omega) = \frac{2J_1(S^{1/2}4NV\sqrt{2}\,I)}{S^{1/2}4NV\sqrt{2}I} \tag{18}$$

where N is the number of fiber coils, V the Verdet constant of silica (rad/A) and I the rms current.

The experimentally obtained data and theoretical expression are plotted in Fig. 14 as a function of signal current. There is good agreement between the experimental and theoretical data, indicating that the sensor output can be electronically relinearized to give a linear accurate output to currents >1 kA.

V. Optimized Sensor Performance

The minimum detectable current in the prototype current sensor was detection shot-noise limited at the low frequencies measured. However, owing to the low power output from the SLD employed and excess optical losses, the potential high sensitivity of the sensor was not achieved. In this section a more realistic power budget is developed for the sensor and the minimum detectable current is then evaluated in terms of total receiver noise. The current monitor frequency response is calculated as a function of coiled fiber length. Finally these factors are combined to predict the maximum current sensitivity which can be achieved in a given measurement bandwidth with a fully optimized sensor.

A. Received Power

The power available from commercial SLD's is ~ 5 mW, of which about 1 mW can be launched into the fiber. Allowing for losses at the beamsplitters and fiber indicates a conservative received power P_R of 100 μW.

B. Noise Sources

A transimpedance amplifier employing a Si-FET front-end gives superior performance up to ~ 100 MHz, beyond which advantages may be gained using a bipolar front end [39], [40]. We restrict our analysis to a transimpedance amplifier with Si-FET front end having a capacitance of 3 pF, and transconductance of $\approx$ 5 mS. The silicon p-i-n photodiode is assumed to have a capacitance of 1.5 pF, a responsivity η of 0.7 A/W and negligible leakage current.

As two preamplifiers are employed there are two Johnson noise currents i_j and two FET noise current i_{FET} contributions to total noise which is then given by:

$$i_{TOT} = (i_s^2 + 2i_{FET}^2 + 2i_j^2)^{1/2} \tag{19}$$

where i_s is the detector shot noise current which is independent of the power split between the two detectors. Using the well-known expressions for noise currents [39], [40] we find that the Johnson noise contribution is negligible if the feedback resistor employed is greater than ~ 5 kΩ and the FET noise does not become comparable to the detector shot noise until approximately 100 MHz. However, above this frequency it dominates and therefore the noise increases with bandwidth to the power 3/2.

C. Noise Equivalent Current

In the small signal case the electronic signal processing calculates the ratio:

$$P = \frac{I_1 - I_2}{I_1 + I_2} \approx 2\theta \tag{20}$$

where

$$\theta = 2NVIs. \tag{21}$$

The noise equivalent current I_{min} (the current at which the signal-to-noise ratio is unity) is then given by:

$$I_{min} = \frac{1}{4NVs}\frac{\text{noise}}{\eta P_r}\ \text{A}. \tag{22}$$

D. Bandwidth-Limited Operation

The bandwidth of the current sensor is limited by the fact that the instantaneous value of current changes during the time taken for the light to propagate through the fiber coil. Thus, the light emerging from the coil, length l at an instant in time, t will have accumulated an optical rotation given by the integral of the current over the time of propagation of that portion of light, that is from $t - 2ln/c$ to t where n is the refractive index. The optical rotation induced by a sinusoidal current of amplitude a and an-

gular frequency ω is thus:

$$\theta(\omega) = \int_{t-2ln/c}^{t} ka \sin \omega t' \, dt' \qquad (23)$$

where k is a constant relating the optical rotation to current. Integrating we obtain:

$$\theta(\omega) = 2\frac{ka}{\omega} \sin\left(\omega t - \frac{ln}{c}\right) \sin\left(\frac{ln\omega}{c}\right). \qquad (24)$$

From this equation we see that the optical signal has a constant time delay of ln/c and its amplitude varies with frequency as a sinc function. Thus the optimum fiber length l_{opt} for a given frequency response F_0 is given by

$$l_{opt} = \frac{1}{4}\frac{c}{nF_0}. \qquad (25)$$

Thus for a 10 MHz bandwidth the optimum fiber length is 5 m.

E. Projected Sensor Response

Equations (22) and (25) for the noise equivalent current and optimized fiber length for a given bandwidth have been combined to plot the minimum detectable current in a given bandwidth in Fig. 15. The curves are plotted for two realizable coil diameters of 10 and 100 mm and assuming a practical fiber length limit of 100 m, which corresponds to 3200 turns of a 10 mm-diam coil.

From this figure we see that in the low-frequency region (<300 kHz), the fiber length is limited to 100 m not by bandwidth considerations, but by practical considerations. The minimum detectable current is limited by detection shot noise and thus increases with the square root of the bandwidth. Typically for a 1 kHz measurement bandwidth a maximum sensitivity of 100 μA rms is obtained for a 10 mm coil.

For higher frequencies (1–100 MHz) the sensor is still detection shot-noise limited. However, since the maximum fiber length has to be reduced to cater for the increased bandwidth, the minimum detectable current increases with bandwidth to the power 3/2. Thus for a 10 MHz bandwidth a maximum sensitivity of 0.3 A rms is projected for a 10 mm coil.

Above 100 MHz the minimum detectable current increases with bandwidth to the power 5/2, since the detection noise is now dominated by the FET channel noise in the preamplifier.

VI. Conclusion

A quasi-circularly birefringent fiber has been developed using spun bow-tie fiber and modeled using Jones calculus. Three optical geometries employing this fiber for current monitoring have been proposed and evaluated to overcome the intrinsic thermal drift of the fiber birefringence.

A maximum current sensitivity of 100 μA rms $Hz^{-1/2}$ for the single-pass configuration was obtained. However, this configuration remained prone to thermal and mechanical effects and was sensitive to light-source wavelength instability.

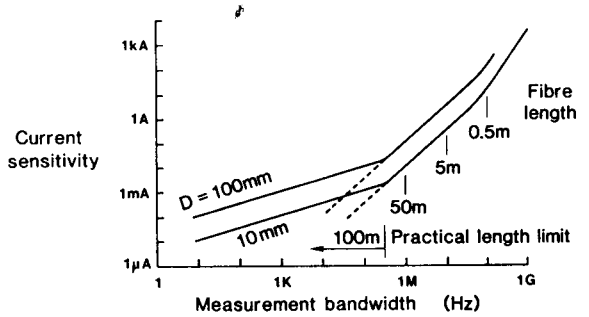

Fig. 15. Calculated current sensitivity of SEB fiber current sensors assuming the maximum fiber length permitted for a given bandwidth is used. The curve is drawn for 10-mm and 100-mm fiber coils and is restricted to a practical fiber length of 100 m.

The use of an orthoconjugate reflector was found to stabilize the fiber-current-sensor response, but had a number of practical disadvantages.

The reflect-back optical configuration using a broadband optical source is a simple and inexpensive solution which provides excellent stability. The theory describing this sensor has been developed and experimentally verified. A prototype 100-turn fiber sensor was constructed and found to have a measurement repeatability of ± 0.5 percent and a temperature drift of 0.05 percent/C°. As a consequence of using the spun birefringent fiber, the current sensor was insensitive to external loading and could be wound as small as 13 mm in diameter with only a 1-percent reduction in sensitivity. The fiber was also found to be approximately 40-dB less vibration sensitive than conventional fiber. A maximum current sensitivity of 1 mA rms $Hz^{-1/2}$ and a large signal response of 450-A rms were demonstrated, giving the device a dynamic range of 113 dB. With minor improvements we expect to improve the maximum sensitivity to 100 μA rms $Hz^{-1/2}$ and the dynamic range to 140 dB.

The ability to wind small fiber coils while retaining high current sensitivity allows short fiber lengths to be used and high bandwidths are therefore possible. Compact all-dielectric current sensors with milliampere sensitivity in the megahertz range can be projected.

Acknowledgment

The authors would like to thank L. Li for helpful discussions and R. Bailey, G. Wylangowski, and R. D. Birch for assistance in fiber fabrication.

References

[1] A. M. Smith, "Polarisation and magnetooptic properties of single-mode optical fibre," *Appl. Opt.*, vol. 17, no. 1, pp. 52–56, Jan. 1978.
[2] A. Papp and H. Harms, "Magnetooptical current transformer. 1: Principles," *Appl. Opt.*, vol. 19, no. 22, pp. 3729–3734, Nov. 1980.
[3] H. Aulich, W. Beck, N. Douklias, H. Harms, A. Papp, and H. Schneider, "Magnetooptical current transformer. 2: Components," *Appl. Opt.*, vol. 19, no. 22, pp. 3735–3740, Nov. 1980.
[4] H. Harms and A. Papp, "Magnetooptical current transformer. 3: Measurements," *Appl. Opt.*, vol. 19, no. 22, pp. 3741–3745, Nov. 1980.
[5] J. N. Ross, "The rotation of the polarisation in low birefringence

monomode optical fibres due to geometric effects," *Optical Quantum Electron.*, vol. 16, pp. 455-461, 1984.
[6] A. J. Barlow, J. J. Ramskov-Hansen, and D. N. Payne, "Birefringence and polarisation mode-dispersion in spun single-mode fibres," *Appl. Opt.*, vol. 20, no. 17, pp. 2962-2968, Sept. 1981.
[7] D. N. Payne, A. J. Barlow, and J. J. Ramskov-Hansen, "Development of low- and high-birefringence optical fibres," *IEEE J. Quantum Electron.*, vol. QE-18, no. 4, pp. 477-488, Apr. 1982.
[8] A. J. Barlow and D. N. Payne, "Polarisation maintenance in circularly-birefringent fibres," *Electron. Lett.*, vol. 17, no. 11, pp. 388-389, May 1981.
[9] A. J. Barlow, J. J. Ramskov-Hansen and D. N. Payne, "Anisotropy in spun single-mode fibres," *Electron. Lett.*, vol. 18, no. 5, pp. 200-202, Mar. 1982.
[10] R. Ulrich and A. Simon, "Polarisation optics of twisted single-mode fibres," *Appl. Opt.*, vol. 18, no. 13, pp. 2241-2251, July 1979.
[11] R. Ulrich, S. C. Rashleigh, and W. Eickhoff, "Bending-induced birefringence in single-mode fibres," *Opt. Lett.*, vol. 5, no. 6, pp. 273-275, June 1980.
[12] S. C. Rashleigh and R. Ulrich, "Magnetooptic current sensing with birefringent fibres," *Appl. Phys. Lett.*, vol. 34, no. 11, pp. 768-770, June 1979.
[13] A. M. Smith, "Single-mode fibre pressure sensitivity," *Electron. Lett.*, vol. 16, no. 20, pp. 773-774, Sept. 1980.
[14] J. Lizet, S. Valette, and D. Langeac, "Reduction of temperature and vibration sensitivity of a polarimetric current sensor," *Electron. Lett.*, vol. 19, no. 15, pp. 578-579, July 1983.
[15] G. W. Day and S. M. Etzel, "Annealing of bend-induced birefringence in fibre current sensors," in *Proc. IOOC-ECOC*, 1985, pp. 871-874.
[16] S. C. Rashleigh, "Origins and control of polarisation effects in single-mode fibres," *J. Lightwave Technol.*, vol. LT-1, no. 2, pp. 312-331, June 1983.
[17] A. D. Kersey and D. A. Jackson, "Current sensing utilising heterodyne detection of the Faraday effect in single-mode optical fiber," *J. Lightwave Technol.*, vol. LT-4, no. 6, pp. 640-643, June 1986.
[18] A. M. Smith, "Optical fibres for current measurement applications," *Opt. Laser Technol.*, vol. 12, no. 1, pp. 25-29, Feb. 1980.
[19] A. M. Smith, "Optical fibre current measurement device at a generating station," *Proc. Soc. Photo-Opt. Instrum. Eng.*, vol. 236, pp. 352-357, 1980.
[20] P. Meyrueix, P. Tatin, and D. Chatrefou, "Capteur de courant a effet Faraday: un prototype performant a fibre optique monomode," *Rev. Generale d'Electricite*, pp. 24-29, June 1986.
[21] S. R. Norman, D. N. Payne, M. J. Adams, and A. M. Smith, "Fabrication of single-mode fibres exhibiting extremely low polarisation birefringence," *Electron. Lett*, vol. 15, pp. 309-311, 1979.
[22] A. J. Rogers, "Optical-fiber current measurement," in *Proc. Sixth Eur. Fibre Optic Commun. and Local Area Networks Exposition*, Amsterdam, The Netherlands, 1988, pp. 203-211.
[23] L. Jeunhomme and M. Monerie, "Polarisation-maintaining single-mode fibre cable design," *Electron. Lett.*, vol. 16, pp. 921-922, 1980.
[24] M. P. Varnham, R. D. Birch, and D. N. Payne, "Helical-core circularly birefringent fibres," in *Proc. IOOC-ECOC* (Venice, Italy), 1985, pp. 135-138.
[25] R. D. Birch, "Fabrication and characterization of circularly birefringent helical fibres," *Electron. Lett.*, vol. 23, no. 1, pp. 50-52.
[26] L. Li, J. R. Qian, and D. N. Payne, "Current sensors using highly birefringent bow-tie fibres," *Electron. Lett.*, vol. 22, no. 21, pp. 1142-1144, 1986.
[27] L. Li, J. R. Qian, and D. N. Payne, "Miniature multiturn fibre current sensors," *Int. J. Optical Sensors*, vol. 2, no. 1, pp. 25-31, 1987.
[28] R. D. Birch, M. P. Varnham, D. N. Payne, and K. Okamoto, "Fabrication of a stress-guiding optical fibre," *Electron. Lett.*, vol. 19, no. 21, pp. 866-867, 1983.
[29] A. Ourmazd, M. P. Varnham, R. D. Birch, and D. N. Payne, "Thermal properties of highly birefringent optical fibres and preforms," *Appl. Opt.*, vol. 22, no. 15, pp. 2374-2379, 1983.
[30] R. C. Jones, "A new calculus for the treatment of optical systems (Parts I-III)," *J. Opt. Soc. Amer.*, vol. 31, pp. 488-503, 1941.
[31] J. Noda, T. Hosaka, Y. Sasaki, and R. Ulrich, "Dispersion of Verdet constant in stress-birefringent silica fibre," *Electron. Lett.*, vol. 20, no. 22, pp. 906-908, 1984.
[32] R. I. Laming, D. N. Payne, and L. Li, "Current monitor using elliptical birefringent fibre and active temperature compensation," *Proc. SPIE, Int. Soc. Opt. Eng.*, vol. 798, pp. 283-287, 1987.
[33] A. Dandridge and H. F. Taylor, "Correlation of low-frequency intensity and frequency fluctuations in GaAlAs lasers," *IEEE J. Quantum Electron.*, vol. QE-18, no. 10, pp. 1738-1750, 1982.
[34] K. Kikuchi and T. Okoski, "Measurement of spectra and correlation between FM and AM noises in GaAlAs lasers," *Electron. Lett.*, vol. 19, pp. 812-813, 1983.
[35] C. Edge and W. J. Stewart, "Measurement of nonreciprocity in single-mode optical fibres,"in *Tech. Dig. IEE Colloq. Optical Fibre Measurements*, no. 1987/55, May 1, 1987.
[36] S. C. Rashleigh and R. Ulrich, "Optical fibre current measurement apparatus," Patent Application nos. DE 3116149 and GB 2100018.
[37] R. I. Laming, D. N. Payne, and L. Li, "Sensitive miniature optical fibre current monitor with passive temperature stabilization," presented at Workshop on Role of Optical Sensors in Power Systems Voltage and Current Measurements, Gaithersburg, MD, Sept. 16-18, 1987.
[38] R. I. Laming, D. N. Payne, and L. Li,"Compact optical fibre current monitor with passive temperature stabilization," in *Proc. OFS* (New Orleans, LA), Jan. 27-29, 1988, pp. 123-128.
[39] J. L. Hullett and T. V. Muoi, "A feedback receive amplifier for optical transmission systems," *IEEE Trans. Commun.*, vol. 24, pp. 1180-1185, 1976.
[40] J. E. Goell, "Input amplifiers for optical PCM receivers," *Bell Syst. Tech. J.*, vol. 53, no. 9, pp. 1771-1793, 1974.

*

Richard I. Laming was born in Sheffield, England, on March 12, 1962. He received a first class honors degree in mechanical engineering from Nottingham University in 1983.

After a brief spell developing engine management systems for the Ford Motor Company, Ltd., he joined the Optical Fibre Group, The University, Southampton, U.K., in October 1984 where he is now the Pirelli Research Fellow. His research interests have included fiber vibration and current sensors, while his recent work has centered on the erbium-doped fiber amplifier.

In 1989 he received the Marconi International Fellowship, Young Scientist of the Year Award.

*

David N. Payne was born in Lewes, England, on August 13, 1944, and educated in Central Africa. He received the B.Sc. degree in electrical engineering, the diploma in quantum electronics, and the Ph.D. degree from the University of Southampton, England.

In 1971 he was appointed the Pirelli Research Fellow in the Department of Electronics, University of Southampton, and in 1977 became a Senior Research Fellow. He is currently Research Reader and directs the Optical Fibre Group, consisting of some 40 members. Since 1969 his research interests have been in optical communications and have included preform and fiber fabrication techniques, optical propagation in multimode and single-mode fibers, fiber and preform characterization, wavelength-dispersive properties of optical fiber materials, optical transmission measurements, and fiber devices. He has published over 150 papers and holds 11 patents. Currently his main fields of interest are special fibers, fiber lasers and devices, fiber sensors, and optical transmission.